Brilliant Engineering 2 (2020) 21-24

Brilliant Engineering

www.acapublishing.com

RESEARCH ARTICLE

The Structural and Mechanical Properties of MoS2-TiB2 Coated on AA7075 Produced by Powder Metallurgy Method

Taha Alper Yılmaz[1], Ayşenur Keleş[2], Güzide Meltem Lüle Şenöz[1], Yaşar Totik[2], İhsan Efeoğlu[2]
[1] Department of Metallurgical Engineering, Atatürk University, Erzurum, Turkey
[2] Department of Mechanical Engineering, Atatürk University, Erzurum, Turkey

Abstract

AA7075 Al alloys are widely used in the aerospace industry. However, the mechanical properties of these alloys are insufficient in space conditions. AA7075 Al alloy is produced by powder metallurgy method due to the good wear properties. Then AA7075 Al alloys have to be adapted to mechanical properties MoS2-TiB2 composite films are deposited. MoS2-TiB2 composite films were grown on powder metal substrate using CFUBMS method in three different MoS2 target currents. Structural properties of composite films were analyzed by SEM, XRD and XPS methods. The mechanical properties of the films are carried out by microhardness and scratch tester. The best grade value of AA7075 powder metal alloy was made with 800MPa pressing pressure and increased from 2.61g/cm3 to 2.72g/cm3 after sintering. The highest hardness was obtained at the lowest MoS2 target voltage of 4.7GPa. The highest critical load value was obtained as 26N at the highest MoS2 target voltage.

Keywords: Powder metallurgy, CFUBMS, MoS2-TiB2 composite films, hardness, scratch.

1.Introduction

Powder metallurgy (PM) method can produce materials of highly fine grain, uniform microstructure and good wear properties [1]. Besides that it enables the metallic materials composed from different components of efficient unique property combinations [2]. One of the main types of materials produced by this method is aluminum (Al) alloys. Al and its alloys have good corrosion resistance, low density, high electrical conductivity and strength. In particularly, Al alloys of the 7XXX series exhibit high strength because they contain alloying elements such as zinc, magnesium and copper [3]. These alloys are also used in armor plates, transportable bridges, girders, vehicles for military and railway transport systems, storage tanks, naval and marine applications [4]. Due to the weak tribological properties of the alloy, surface properties are required to be improved. Especially AA7075 alloy has good abrasive and wear resistance. Therefore, solid lubricants have been used to improve the tribological properties of the AA7075 alloy. Solid lubricants are frequently used in areas where tribological properties are important such as high vacuum, high temperature, aviation and space where traditional materials and liquid lubricants cannot achieve the desired performance levels. MoS2, TiB2, h-BN, graphite etc. coatings are most commonly used as solid lubricants. As a comparison was made between the solid lubricants, in the space industry MoS2 and TiB2 are most attractive films [5]. However, the lubrication properties of MoS2 are deteriorated in the moist air due to oxidation of MoO3 [6, 7]. As very well known, while friction coefficient increases, adhesion and coating life decreases. For this reason, many materials such as metal (Au, Ti, Ta etc.) or ceramics (TiB2) is added to remove deterioration in MoS2 coatings [8-12]. Scratch test and reciprocating multi-pass test are carried out to determine the adhesion and wear life of coatings, respectively [13]. To deposit solid lubricants, magnetron sputtering is commonly used in industry. Films can be coated with uniform, better adhesion and coating life by magnetron sputtering [14].

In this study, AA7075 were produced by PM. MoS2-TiB2 composite films were deposited on AA7075 produced by powder metallurgy using Closed Field Unbalanced Magnetron Sputtering (CFUBMS). The structural and chemical properties of the coated films were characterized by XRD, SEM and XPS. The mechanical properties of AA7075 samples and composite films were determined by microhardness test, scratch tester and reciprocating multi-pass test.

2. Experimental Methods

A commercially, atomized and spherical AA7075 powder alloy with chemical composition is given in Table 1.

Table 1. The chemical composition of AA7075

Elements	Al	Cu	Mg	Zn	Others
wt. %	89.7	1.2	2.1	6.8	0.2

The bulk material has 20mm diameter with 5 mm thickness was produced from aluminum powder that have 74μm size by using a uniaxial pressing method. In order to obtain optimum density of bulk material, pressing processes were performed by at the different pressing pressure values (700-900 MPa).

Before coating, AA7075 substrates were polished to Ra≈0.1μm. MoS2-TiB2 composite films were grown on AA7075 and glass using CFUBMS with dc power supply. The schematic picture of CFUBMS was given

*Corresponding Author: cebel@cebel.com
(T.A.Yılmaz)
Received 18 Dec 2019 Revised 18 Dec 2020 Accepted 18 Dec 2019
Brilliant Engineering 2 (2020) 21-24

https://doi.org/10.36937/ben.2020.002.004

Fig.1. In the process, 2 Ti targets, 1 MoS2 target and 1TiB2 target were used. For plasma and ionization, Ar gas was used. Before the process, ion cleaning was carried out in 20 min. with -600V to eliminate contamination. To improve adhesion, Ti interlayer was coated at Ti current of 5A, substrate bias of -150V and deposition time of 5 min. The deposition parameters were given in Table 2. After Ti interlayer, MoS2-TiB2 composite films were deposited under different MoS2 target current values.

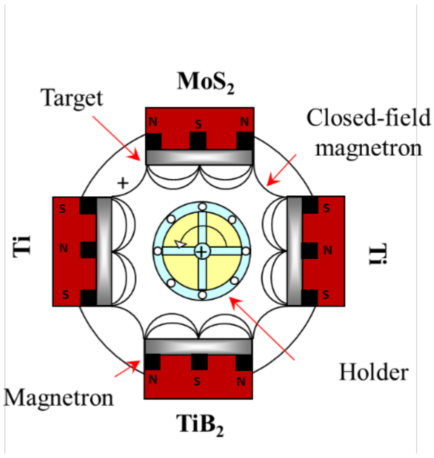

Figure 1. The schematic picture of CFUBMS

Table 2. The deposition parameter

	R1	R2	R3
The variable parameter			
MoS_2 target current(A)	0.5	1	1.5
The constant parameters			
TiB_2 target current(A)	4		
Substrate voltage (-V)	70		
Time (min)	90		
Coating pressure (Pa)	0.33		

The film thickness and microstructure were observed using SEM (Zeiss Sigma 300). The crystallographic structure was obtained using XRD (Rigaku-2200 D/Max) a scan range of 10-60°. The elemental analysis was determined using XPS (Specs-Flex). The mechanical properties of MoS2-TiB2 composite films were carried out using microhardness test (Buehler) with Knoop indenter at 10gf in 15s and scratch test (Revetester CSM Instruments) under speed of 10mm/min and loading rate of 100N/min.

3. Results and Discussion

For the production of the substrate, the pressing pressure is optimally determined. Five different pressing pressures were used to determine the closest value to the theoretical density. In cold pressing processes, samples were obtained under pressures of 700, 750, 800, 850 and 900MPa. The density values of all samples were measured with the Archimedes principle. Table 3 shows the density value of AA7075 samples at different pressing pressures. Then, when the density measurements of the samples obtained from each pressing pressure were carried out, the closest value to the theoretical density gave a pressure of 2,61g /cm3 under 800MPa.

Sintering process was started after pressing operations. Samples with the most optimum density value (800MPa) were subjected to sintering. The sintering process was carried out under the atmosphere of Ar to prevent oxidation. All samples were sintered at 590 °C for 1 hour. After the sintering process, the density of the highest green density of 2,61g/cm3 increased to 2,72g/cm3 in the final case. Thus, substrate production was performed by PM method with density value close to the bulk sample.

Table 3. The green density of the AA7075

Pressing Pressure (MPa)	**Green Density (g/cm^3)**
700	2,45
750	2,51
800	**2,61**
850	2,55
900	2,52

The elemental contents, hardness values are summed up in Table 4.

	% at.				**Hardness (GPa)**
	S	B	Mo	Ti	
R1	37.510	42.029	17.599	2.862	4.7
R2	37.425	40.220	21.485	0.870	3.5
R3	35.154	41.143	22.122	1.581	3

The film thickness and microstructure of MoS2-TiB2 composite films are given in Fig. 2. According to Fig. 2, all films have dense microstructure due to CFUBMS. The film thickness values and grain size sputter rate. The sputter rate increases in direct proportion to the target current [15].

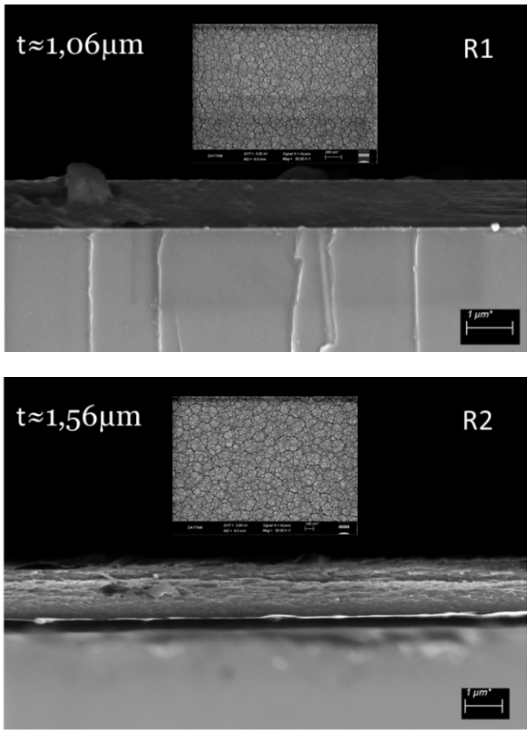

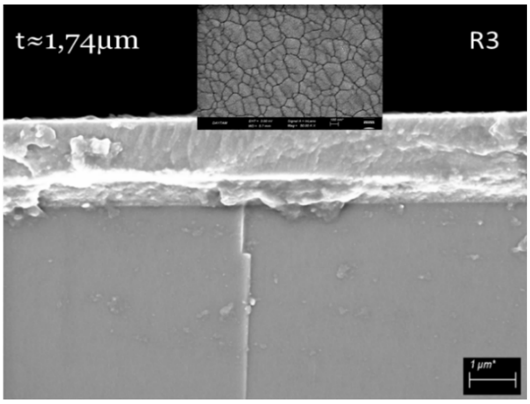

Figure 2. The film thickness and microstructure of MoS2-TiB2 composite films

The XRD graph of MoS2-TiB2 composite films is given in Fig. 3. All films have TiB2 (001), TiB2 (101), MoS2 (100) and MoS2 (202) phases.

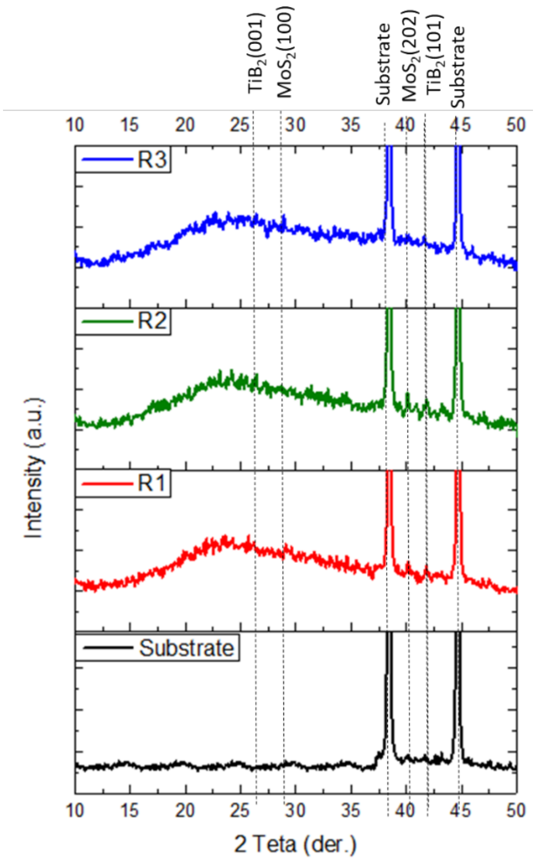

Figure 3. XRD graph for MoS2-TiB2 composite films

The XPS graph of MoS2-TiB2 composite films is given in Fig. 4. The graph is showed that the increasing MoS2 target current, Mo and S amounts increase. The target current affects the Mo and S contents. Moreover, Mo and S amount negatively affect the hardness value [16]. Therefore, R1 film has the highest hardness value due to low MoS2 content. Also, the decreasing target current reduces the grain size and increases the hardness value [17].

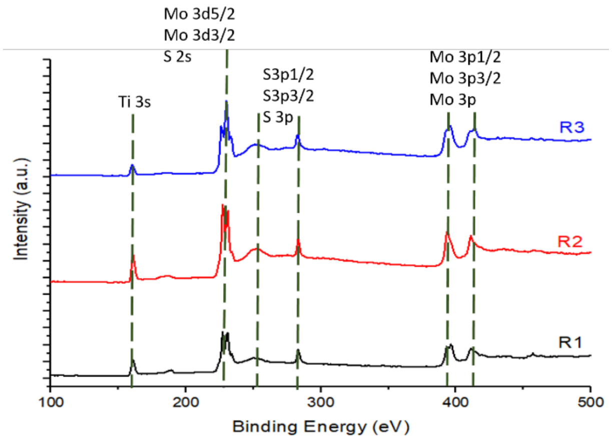

Figure 4. XPS graph for MoS2-TiB2 composite films

The scrath graphs and pictures of MoS2-TiB2 composite films are given Fig. 5-7. The critical load values are 15N, 20N and 26N for R1, R2 and R3, respectively. When compared critical load values, the highest critical load value has been obtained from the lowest hardness value. The critical load has increased with

increasing film thickness (see Fig.2) and decreasing hardness [18].

A comparison has been made between scratch pictures, for R1 film, edge failures have started after 5N. Also, there is buckling in the scratch track. After 10N, the adhesive failure has been observed in the scratch track [19]. For R2 film, chipping has occurred in the edges after 5N. The adhesive failures and gross spallation have happened after 15N. For R3 film, adhesive failures have been observed in all pictures. The amount of adhesive failures has increased with increasing load value.

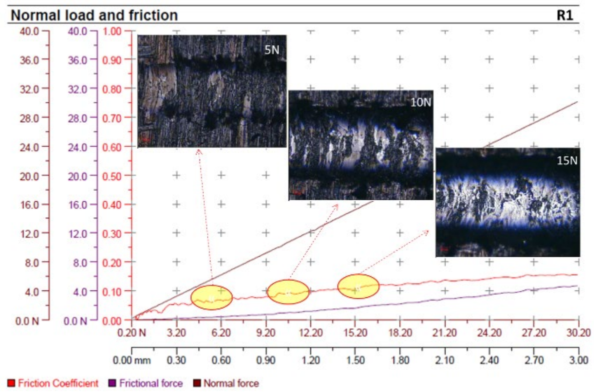

Figure 5. The scratch results for R1

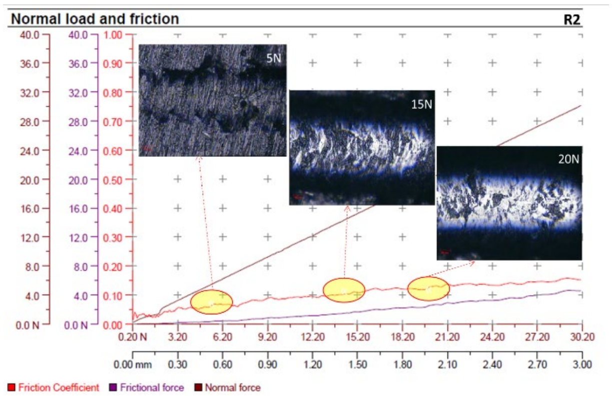

Figure 6. The scratch results for R2

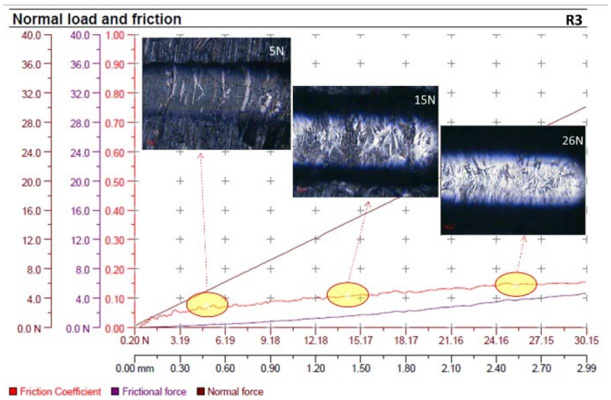

Figure 7. The scratch results for R3

4. Conclusions

The maximum green and sintering intensity was obtained from 800 MPa pressing pressure. So, AA7075 with the maximum green intensity was chosen as a substrate material. MoS2-TiB2 composite films were grown on AA7075 substrates using CFUBMS with dc power supply. The maximum thickness value was 1.74μm. The thickness values increased with increasing MoS2 target current. The maximum hardness (4.7GPa) was measured from the lowest MoS2 target current. The increased film thickness caused decreasing in hardness value. Besides, the grain size increased with decreasing hardness value. The maximum critical load was measured as 26N. The critical load increased with decreasing microhardness.

References

[1] T.R. Prabhu, Effect of Compaction Load and Sintering Temperature on Tribological and Mechanical Behavior of Ni/SiC/MoS2 Composites, J. Mater. Eng. Perform. 25 (4) (2016) 1436-1445.

[2] I. Pokorska, Deformation of powder metallurgy materials in cold and hot forming, J Mater Process Tech 196 (1) (2008) 15-32.

[3] R.H. Estrada-Ruiz, R. Flores-Campos, J.M. Herrera-Ramirez, R. Martinez-Sanchez, Mechanical properties of aluminum 7075-Silver nanoparticles powder composite and its relationship with the powder particle size, Adv Powder Technol 27 (4) (2016) 1694-1699.

[4] P. Vijaya Kumar, G. Madhusudhan Reddy, K. Srinivasa Rao, Microstructure and pitting corrosion of armor grade AA7075 aluminum alloy friction stir weld nugget zone – Effect of post weld heat treatment and addition of boron carbide, Defence Technology 11 (2) (2015) 166-173.

[5] Ö. Baran, F. Bidev, H. Çiçek, L. Kara, İ. Efeoğlu, T. Küçükömeroğlu, Investigation of the friction and wear properties of Ti/TiB2/MoS2 graded-composite coatings deposited by CFUBMS under air and vacuum conditions, Surface and Coatings Technology 260 (2014) 310-315.

[6] I. Efeoglu, Co-sputtered Mo : S : C : Ti : B based coating for tribological applications, Surf Coat Tech 200 (5-6) (2005) 1724-1730.

[7] T. Spalvins, LUBRICATION WITH SPUTTERED MOS2 FILMS - PRINCIPLES, OPERATION, AND LIMITATIONS, J. Mater. Eng. Perform. 1 (3) (1992) 347-352.

[8] J.R. Lince, M.R. Hilton, A.S. Bommannavar, Metal Incorporation in Sputter-Deposited Mos2 Films Studied by Extended X-Ray-Absorption Fine-Structure, J Mater Res 10 (8) (1995) 2091-2105.

[9] I. Efeoglu, F. Bulbul, Effect of crystallographic orientation on the friction and wear properties of MoxSy–Ti coatings by pulsed-dc in nitrogen and humid air, Wear 258 (5) (2005) 852-860.

[10] X. Wang, Y.M. Xing, S.L. Ma, X.L. Zhang, K.W. Xu, D.G. Teer, Microstructure and mechanical properties of MOS2/titanium composite coatings with different titanium content, Surf Coat Tech 201 (9-11) (2007) 5290-5293.

[11] X. Zhang, B. Prakash, W. Lauwerens, X. Zhu, J. He, J.P. Celis, Low-Friction MoSxCoatings Resistant to Wear in Ambient Air of Low and High Relative Humidity, Tribology Letters 14 (2) (2003) 131-135.

[12] F. Bidev, Ö. Baran, E. Arslan, Y. Totik, İ. Efeoğlu, Adhesion and fatigue properties of Ti/TiB2/MoS2 graded-composite coatings deposited by closed-field unbalanced magnetron sputtering, Surface and Coatings Technology 215 (2013) 266-271.

[13] N. Panich, Y. Sun, Chapter 10 - Mechanical Characterization of Nanostructured TIB2 Coatings Using Microscratch Techniques, in: S. Sinha (Ed.) Tribology and Interface Engineering Series, Vol. 51, Elsevier, 2006, pp. 210-222.

[14] T. Polcar, A. Cavaleiro, Review on self-lubricant transition metal dichalcogenide nanocomposite coatings alloyed with carbon, Surface and Coatings Technology 206 (4) (2011) 686-695.

[15] T.L. Brzezinka, J. Rao, M. Chowdhury, J. Kohlscheen, G.S.F. Rabinovich, S.C. Veldhuis, J.L. Endrino, Hybrid Ti-MoS2 Coatings for Dry Machining of Aluminium Alloys, Coatings 7 (9) (2017).

[16] R. Gilmore, M.A. Baker, P.N. Gibson, W. Gissler, Preparation and characterisation of low-friction TiB2-based coatings by incorporation of C or MoS2, Surface and Coatings Technology 105 (1) (1998) 45-50.

[17] H. Niakan, C. Zhang, L. Yang, Q. Yang, J.A. Szpunar, Structure and properties of DLC–MoS2 thin films synthesized by BTIBD method, J Phys Chem Solids 75 (12) (2014) 1289-1294.

[18] H. Ichimura, A. Rodrigo, The correlation of scratch adhesion with composite hardness for TiN coatings, Surf. Coat. Technol. 126 (2-3) (2000) 152-158.

[19] S.J. Bull, Failure mode maps in the thin film scratch adhesion test, Tribol Int 30 (7) (1997) 491-498.